

# Bi(2223) Ag sheathed tape $I_c$ and exponent $n$ characterization and modelling under DC applied magnetic field.

Bertrand Dutoit, Mårten Sjöström and Svetlomidir Stavrev  
Swiss Federal Institute of Technology, EPFL-DE-CIRC, 1015 Lausanne, SWITZERLAND

**Abstract**—We use a dual channel digital lock-in to perform electrical measurement of AC losses at power frequencies. A DC magnetic field between 2 and 400 mT is applied with a varying angle from parallel to perpendicular to the tape surface, thus having a complete view of the loss behavior under DC applied field. Furthermore, the same experimental layout is used to acquire time series of current and voltage across the sample. Using a triangular input current, we measure and average the voltage, which then is fitted to a power law  $(I/I_c)^n$ . The measurements are repeated for the mentioned magnetic field and angle range to give the dependencies of  $I_c$  and  $n$  with the field amplitude and angle. For device modeling purposes, we can then express a phenomenological law giving  $I_c$  and  $n$  as a function of the applied magnetic field's intensity and direction.

In superconducting Bi(2223) tapes a power law of the form  $V = V_0 (I / I_c)^n$  can well describe the current-voltage characteristics. An applied DC magnetic field causes a strong diminution of the critical current and of the value of the exponent  $n$ . Since the critical current and exponent of a sample are key parameters to evaluate and compare AC losses within different situations, it is important to know precisely their dependence on the amplitude and direction of the applied field. Several studies [1] were made for either parallel or perpendicular applied fields. In this work, measurements are made for various applied field angles, which means combined parallel and/or perpendicular field components.

## I. INTRODUCTION

The considerable interest in the possibility of using PbBi2223 tapes in a variety of applications make their precise characterization under AC or DC conditions necessary. Recent progress involved achieving long lengths and high current densities, as well as manufacturing cable and device prototypes. Transport and other energy network applications are the largest domain where those tapes can be used. Therefore, losses at the line frequency (50-60 Hz) and under applied magnetic field are a major design factor for many future industrial applications where modelling tools as proposed here are necessary.

## II. EXPERIMENTAL SETUP

### A. Multiple channel digital lock-in

For AC loss evaluation, the electrical characterization method is preferred because once the experimental set-up is correctly tuned, it allows simpler and quicker measurements than traditional calorimetric or magnetization methods. It does not require long samples and is ideal for short ones of 5 to 10 centimeters length. However some difficulties inherent to this electrical method have to be solved. We can mention four of them:

1) *High current and low voltage* are present in the same experimental arrangement. Typically currents of dozens amperes are used and voltages down to dozens nanovolts measured.

Manuscript received september 15, 1998

This work is supported by the Brite-Euram III Program, project BE-1985 - "SACPA"

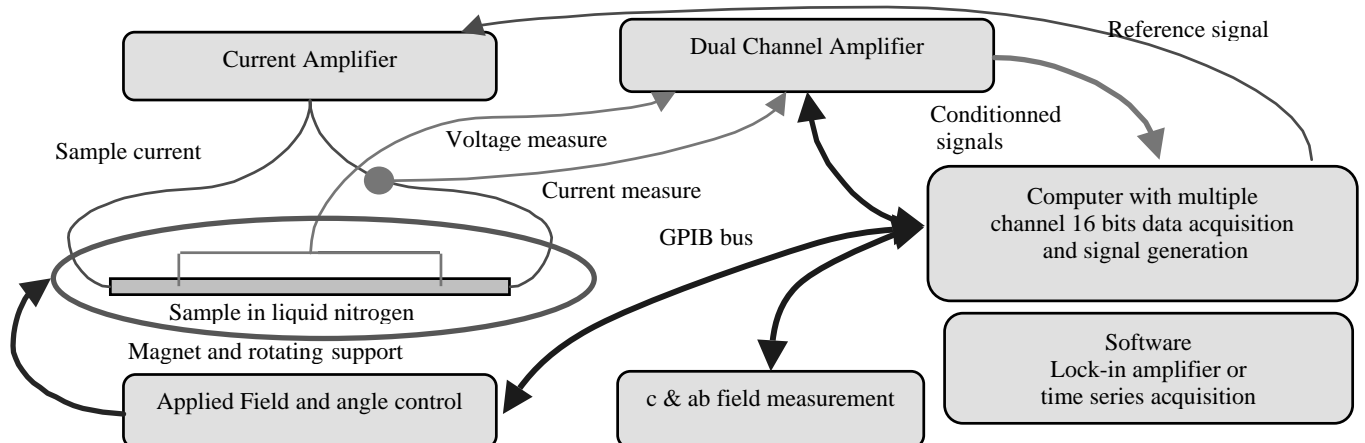


Fig. 1. Experimental setup for time series data acquisition and software lock-in measurement

This implies the use of a high quality, low distortion, low noise current amplifier. Great attention has to be given to prevent coupling between the very-low-voltage measurement circuit and the current circuit.

2) *Phase sensitivity* is the great difficulty of the method. Due to the voltage tap geometry used [2], the inductive component of the voltage is strong. Therefore, any uncertainty on the phase of the current across the sample results in a great error in the resistive component of the voltage. This necessitates the use of a dual channel lock-in to simultaneously measure the actual phase of the current. Thus the phase shift due to the current amplifier does not cause any error.

3) *Great difference between* in phase and in quadrature voltage can lead to serious problems of dynamic reserve of the low-signal amplifier. Due to the great current amplitude and the unavoidable inductive coupling in the sample region, the reactive part of the voltage can be several orders of magnitude higher than the resistive part. The use of a very high dynamic reserve introduces less phase noise than reactive voltage compensation.

4) *Complete characterization* needs simultaneous measurements of more than the first harmonics only. For example, the non-linear inductance near the critical current is present on the third harmonics. Our experimental set-up allows the acquisition of multiple harmonics simultaneously. In fact, we obtain time series on which we can do the desired calculation in order to have the most complete characterization.

### B) Experimental details

Our experimental set-up is represented in Fig. 1. It can be divided into five parts: the current generation circuit with the amplifier, the current measurement circuit, the voltage measurement circuit, the data acquisition system and the data treatment programs.

1) *The current generation circuit.* The current leads are specially configured in order to have a total inductance lower than 0.1  $\mu\text{H}$ , with a total resistance under 0.1  $\Omega$ . This allows driving currents at a few kHz.

2) *The current measurement circuit.* As mentioned above, it is of great importance to know the exact phase of the current across the sample. Therefore, we simultaneously measure the phase and quadrature components of the current using a multiple channel digital lock-in amplifier. The measurement element is composed of twenty low-inductance parallel resistors in a sandwich configuration for a final value of 5  $\text{m}\Omega$  with a calibrated time constant. The shunt voltage is amplified by a factor of ten with a dual channel amplifier. The ground point is chosen in the middle of the shunt in order to have the minimum common mode voltage at the differential input of the amplifier. The output of the amplifier is connected to a differential input of the computer data acquisition board.

3) *The voltage measurement circuit.* To achieve resolutions of the order of 10 nV, the second channel of

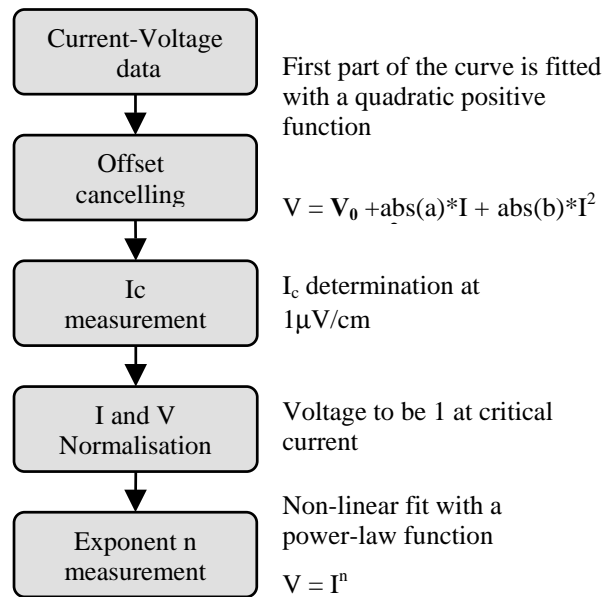


Fig. 2. Data treatment sequence

the amplifier is used for a pre-amplification by a factor of 1000. The grounding of the amplifier is done with a connection to the center of the measured sample. With current lead resistance of the order of 20  $\text{m}\Omega$ , and current in the 10 A region, the voltage drop is about 200 mV. For a resolution of the order of 10 nV the preamplifier should have a common mode rejection ration of 160 dB. No amplifier offers such a characteristic, which means that the amplifier has to be grounded on the sample itself. Very high dynamic reserve and high resolution is preferred to reactive compensation for a better phase accuracy.

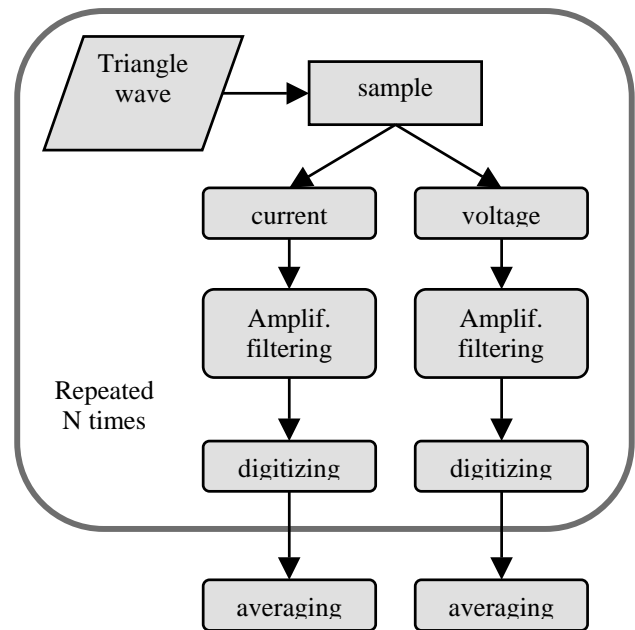


Fig. 3. Data acquisition sequence

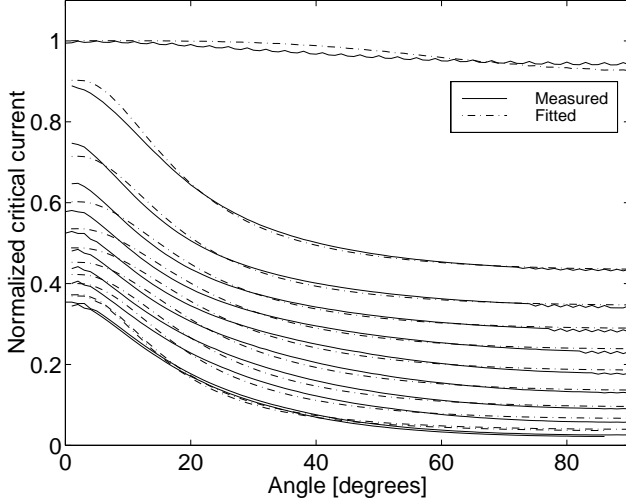


Fig. 4. Normalized critical current  $I_c/I_{c0}$  as a function of the angle of the applied field between 2 and 400 mT, as measured and fitted from eq. (1)

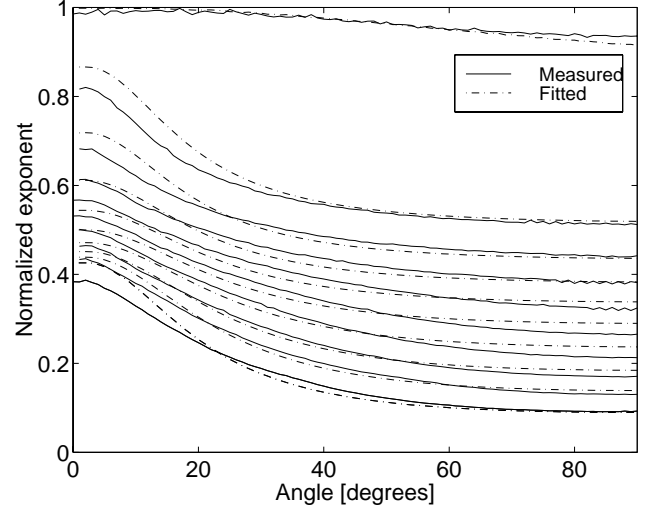


Fig. 5. Normalized exponent  $n/n_0$  as a function of the angle of the applied field between 2 and 400 mT, as measured and fitted from eq. (1)

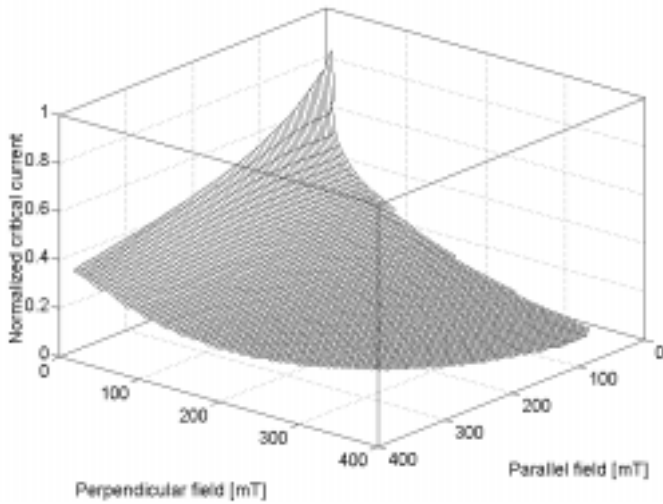


Fig. 6. Normalized critical current  $I_c/I_{c0}$  as a function of the applied field perpendicular to c- and ab-plane between 2 and 400 mT

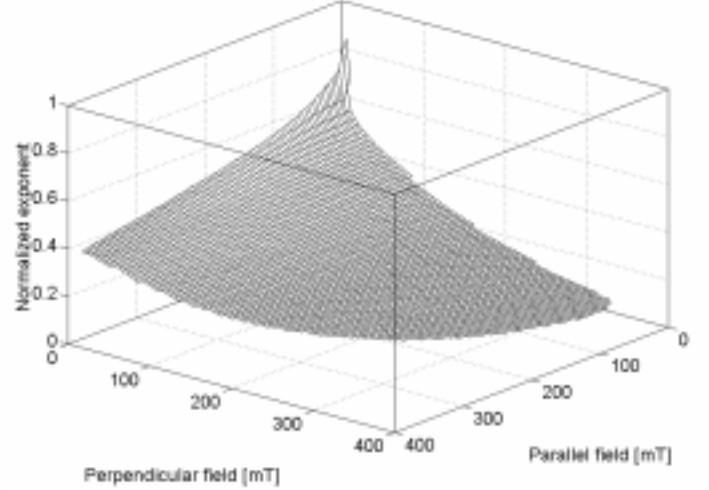


Fig. 7. Normalized exponent  $n/n_0$  as a function of the applied field perpendicular to c- and ab-plane between 2 and 400 mT

4) *The data acquisition system.* Time series data acquisition is made in order to be able to choose the right treatment at any time, which was necessary for this work. A National Instruments PCI-MIO16XE-10 board with high stability 16 bit AD and DA converters is used for digitizing and signal generation. Sampling frequencies are up to 50 kHz in the two channels, while signal generation is done at 200 kHz. The stability of such a device brings ppm resolution [3]

5) *The data treatment programs.* The lock-in technique is used as basic treatment for AC loss measurements. In this case the lock-in is a software program, which does the

harmonic extraction [3]. For the work described in this paper, the data flow is different and is shown in Fig. 2.

### III. DATA ANALYSIS AND RESULTS

As shown in Fig. 3, the data acquisition is done in four steps. To avoid ground loops all signal are measured differentially, which implies the existence of an offset that has to be determined and subtracted.

The first part of the V-I curve is then fitted to a quadratic function with positive coefficients of  $I$  and  $I^2$ . A Levenberg-Marquardt method is used to determine a nonlinear set of coefficients that minimize a chi-square quantity. Afterwards, the critical current is taken as the value corresponding to  $1 \mu\text{V}/\text{cm}$ .

To insure convergence of the power-law fit, it is necessary to normalize the curve so that  $V=1$  at  $I_c$ .

The several measured samples exhibit the same behavior; the results are then normalized respectively to the critical current at zero field  $I_{c0}$  and the exponent at zero field  $n_0$ . Fig. 4 and 5 show the dependence of  $I_c$  and the exponent  $n$  on the angle of applied field with constant magnitude, each curve for a value of the field between 2 and 400 mT. Fig. 6 and 7 show the same results, but as function of simultaneously applied parallel and perpendicular DC fields. As can be seen, the perpendicular field component has greater influence on the  $I_c$  and  $n$  values than the parallel one.

#### IV. DATA FITTING

We have developed an explicit formula that gives the critical current and the exponent  $n$  dependence on the applied field amplitude and direction. We believe it can be useful, for instance, in computer simulations, rather than as a physical explanation.

The expression is based on Kim's model [4] for the dependence of  $I_c$  on  $B$ . At first we consider the  $c$ - and  $ab$ -directions separately. We have noticed that by adding a term in the numerator, a better fit is reached for small fields. In the  $c$ -direction yet another term enables a good fit for the whole measured range.

The two directions must be then related with a smooth function. We have achieved the best result after placing all terms in a single fraction and smoothly decreasing the influence of the  $c$ -direction with a function  $f(\varphi)$ .

$$\frac{I_c(B)}{I_{c0}} = \frac{1 + \left(\frac{B}{B_1}\right)^{p_1} + \left(\frac{B}{B_3}\right)^{p_3} f(\varphi, z_1)}{1 + \left(\frac{B}{B_2}\right)^{p_2} + \left[\left(\frac{B}{B_4}\right)^{p_4} + \left(\frac{B}{B_5}\right)^{p_5}\right] f(\varphi, z_1)} \quad (1)$$

The parameters indexed 1,2 refer to the field in  $ab$ -direction and 3-5 to the  $c$ -direction. The function  $f(\varphi)$  is restricted by  $f(0)=0$ ,  $f(\pi/2)=1$ ; it must be also monotonically increasing, and can be selected in many ways. Measured data are not symmetrical around  $\pi/4$ , so we constructed a function that can be adjusted with an additional parameter  $-z_1$  in eq.(2).

$$f(\varphi, z_1) = \frac{1 - \cos(\alpha(\varphi))}{2} \quad \omega = \frac{z - z_1}{z - 1/z_1} \frac{1 - 1/z_1}{1 - z_1} \quad (2)$$

$$\alpha = \arg(\omega) \quad z = e^{j2\varphi}$$

The parameters in eq. (1) and (2) are identified by minimizing the square error between measured and estimated data. The expression for the exponent

dependence on the field amplitude and direction is similar to eq.(1) and the same structure of the fitted function is used. The results from the fits are shown in Fig. 4, 5 and 8 respectively.

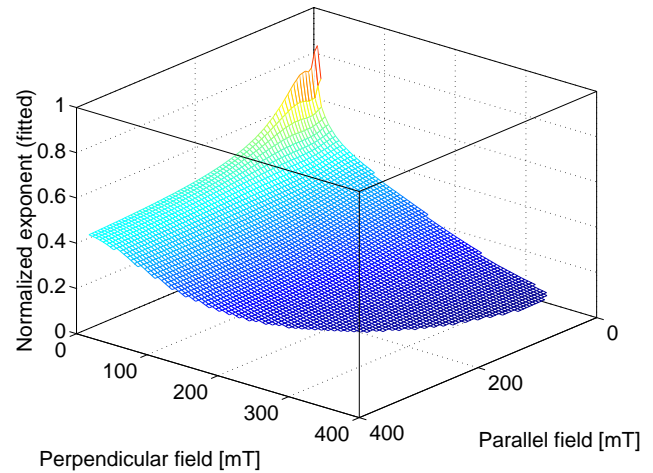


Fig. 8. Exponent  $n$  dependence on the amplitude and direction of  $B$ , as fitted from eq.(1). To be compared with Fig.7 as well.

#### V. CONCLUSIONS

The exponent  $n$  and  $I_c$  exhibit a very similar behavior when increasing the applied DC field amplitude. It is shown that the performance of the tapes under DC applied field is not only characterized by a drastic diminution of the critical current, but also by a corresponding decrease of the exponent value  $n$ . Even for excellent samples, a value of  $n = 20$  at zero field vanishes down to  $n = 2$  or 3 at maximum field. This has to be taken into consideration for AC loss and electromagnetic calculations in new HTS devices. The perpendicular field component has considerably greater influence on the diminution of  $I_c$  and  $n$ . We have suggested a function, which gives the  $I_c$  and  $n$  dependence on the applied field magnitude and angle. It may be used, for example, for modelling purposes in device simulations.

#### REFERENCES

- [1] Grasso G., Hensel B., Jeremie A. and Flükiger R. "Distribution of the transport critical current density in AgBi(2223) tapes produced by rolling" *Physica C* (1994) 241 45-52
- [2] Campbell, A.M. "AC losses in High Tc superconductors" *IEEE trans. Appl. Superconductivity* (1995) 5 682-687
- [3] Probst P-A and Jaquier A. "Multiple-Channel Digital Lock-in Amplifier with ppm Resolution" *Rev. Sci. Instrum.* (1994) 65 747
- [4] Kim Y.B., Hempstead C.F. and Strnad A.R., "Critical persistent currents in hard superconductors", *Phys.Rev.Lett.* 9 (1962) 7, 306-309